ENERGY CALIBRATION OF THE HYCAL DETECTOR USING DOUBLE ARM COMPTON SCATTERING

PRIMEX NOTE 36

Yelena Prok

February 21, 2006

0.1 Objectives

This note describes the procedure for finding the gain correction factors for the crystal modules of the hybrid calorimeter, HYCAL, used in PRIMEX, using the double arm Compton scattering off the (1 % radiation length) carbon target, with the photon beam energy ranges of 2-3 GeV and 4.9-5.5 GeV. The objectives of this procedure are to check the quality of the calibration constants obtained with the dedicated calibration data, to monitor the change of these constants with time, and to compare the results with the LMS monitoring. Two methods of calibration, calibration by iteration, and the "matrix inversion", and the results of calibration are discussed in the sections below.

0.2 Introduction

The gain factors of HYCAL were determined in the beginning and end of the PRIMEX data taking period, using the dedicated calibration scans, during which the photon beam was incident directly on each module. These calibration scans took place on October 9-10 and November 22 of 2004, giving each module the initial (g_i) and final (g_f) gain values. The gain changes were also monitored during the data taking period using the LMS system. The double arm Compton scattering, due to its well defined kinematics, provides another method of monitoring the energy gains of the modules. The dedicated Compron runs were taken periodically throught the run, providing data needed for the calibration procedure. The Compton runs are combined into seven groups, one through seven in the chronological order. It is important to notice, that an incident occured at some point during the run (at run number 5052), when the detector was exposed to an electron beam of 500 nA, after which the affected modules had a significant shift in their gain values (as was demonstrated by this calibration procedure)

Table 1: Compton runs, carbon target

group number	run range	run date	comment
1	4426-4432	Oct 10	low stat
2	4657-4660	Oct 19	
3	4943-4946	Nov 2	
4	4965-4973	Nov 3	
5	5073-5080	Nov 9	rad.inc. at 5052
6	5150-5157	Nov 14	
7	5243-5253	Nov 19	closest to 2nd calib

0.3 Selection of Compton pairs

The Compton events were selected using a number of kinematic and geometric cuts. The pairs of clusters were selected based on the timing coincidences between the tagger and the clusters. The following cuts were applied to the selected pairs:

1. The central opening of the HYCAL (± 4 cm)was cut out.
2. The separation between two clusters was required to be larger than 15 cm
3. We required the minimum energy of the clusters to be larger than 0.5 GeV.
4. Conservation of energy was required: $|(((e_1 + e_2)/e_{beam} - 1.)| < 0.3$
5. Consistency with the Compton kinematics was required: $|E_{beam} - E_{Compton}| < 0.6$, $E_{Compton} = \frac{m_e sin(\theta_\gamma}{2sin^2(\theta_{\gamma 2}/2)tan(\theta_e)} - m_e$, where θ_γ and θ_e are the polar scattering angles of the Compton photon and electron respectively: $\theta_\gamma = atan(\sqrt{x_\gamma^2 + y_\gamma^2}/z)$ and $\theta_e = atan(\sqrt{x_e^2 + y_e^2}/z)$, and $z = 731.23$ cm is the distance from the target to the surface of the crystal part of the detector.

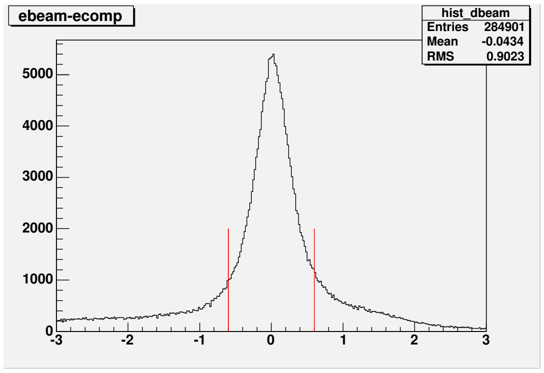

Figure 1: $E_{beam} - E_{compton}$

The electrons and the photons were distinguished using the Detector Match package, where the identification of the VETO-HYCAL simultaneous hit was based on the matching of the x-coordinates.

Some distributions of the resulting electron-photon Compton pairs are shown in Figure 0.3. The $\Delta\phi$ - distribution of the selected γ-e pairs is centered at 179.9 degrees, indicating that most of the selected pairs are coplanar.

Comparison of the angular distributions of the selected photons and electrons with the same quantities generated by kinematic GEANT also indicates that a reasonably clean sample of Compton events is selected.

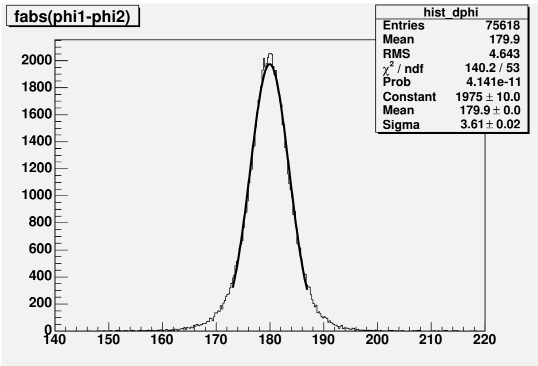

Figure 2: $\Delta\phi$ - distribution of the selected γ-e pairs

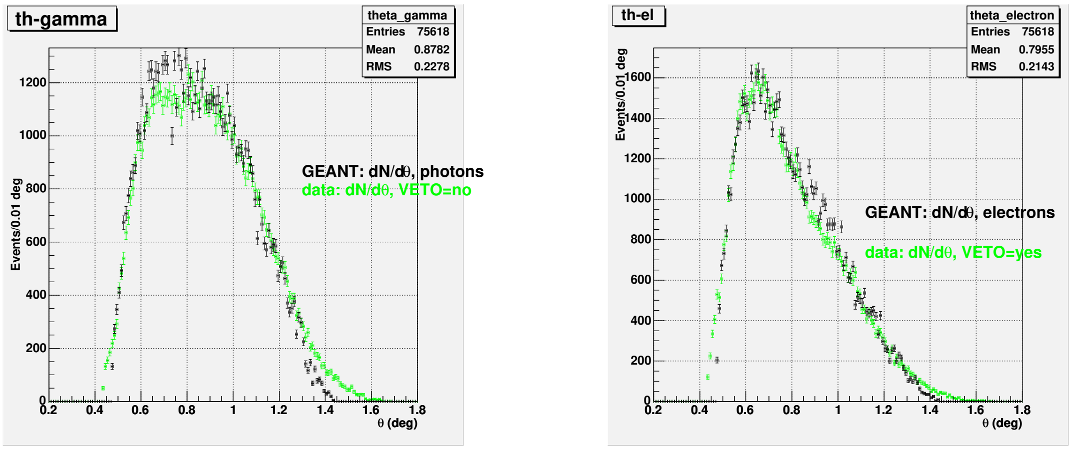

Figure 3: Left:Scattering angle θ_{gamma} for the Compton photons, compared to the same distribution from a kinematic simulation. Right:Scatteing angle θ_{el} for the Compton electrons, compared to the same distribution from a kinematic simulation

0.4 Calibration by iteration: Procedure

The selected pairs of Compton electrons and photons are used to obtain gain correction factors, by comparing detected energies of clusters with the values expected from the Compton kinematics, and the scattering angles. Neglecting the electron mass, expectation values, E_c are the same for the electrons and the photons, and depend only on the beam energy and the scattering angle, θ:

$$E_c = \frac{E_{beam}}{1 + 2 * E_{beam}/m_e * sin^2(\theta/2)} \tag{1}$$

The gain correction value if found by dividing the detected energy of the cluster by the expected value: $gc = E_{measured}/E_c$. The distribution of gc's for each module if fitted with a gaussian function, and the mean value as taken as a correction value, by which the current gain in the calibration database should be divided. An example of

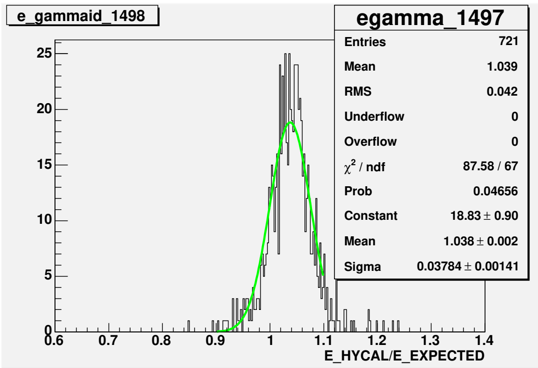

Figure 4: Gain correction factor obtained with Compton photons for module 1498.

such a distribution is shown in Figure 0.4.

0.5 Calibration by iteration: Results

Using the outlined procedure, gain correction factors are found using selected photons, electrons and a mixed sample of particles. Approximately 100-150 counters can be calibrated using the high energy data, with beam energy of 4.9-5.5 GeV. Including the low energy data, accumulated with beam energies of 2-3(?) GeV allowes for greater geometric coverage, increasing the number of modules that can be calibrated to 700. Depending on the module, and the group number (in other words, point in time), the gain correction values range from 0.95 to 1.11. The results obtained using electrons and photons vary sligtly, with the electron sample resulting in the gain correction values systematically 1-3 % higher than the ones obtained with the

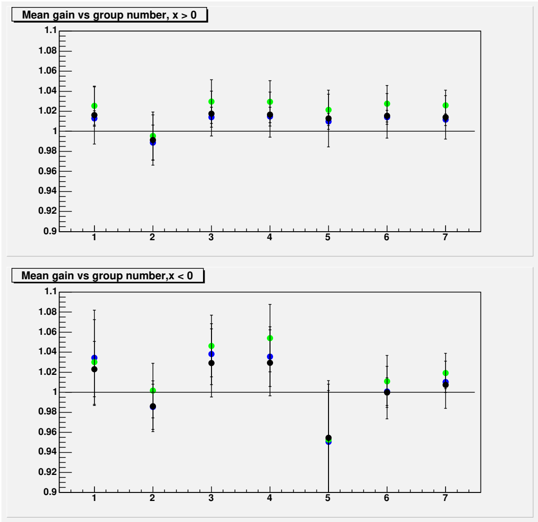

Figure 5: Mean gain correction factors (± RMS) are plotted vs group number: green points indicate electrons, blue-photons, and black- a mixed sample of particles

photon sample. An example of such a distribution is shown in Figure 0.5. A possible explanation of this discrepancy is that the shower depth correction, used in this analysis, was calculated using photons, and might not be adequate for electrons. Another observation made through this study was the left-right asymmetry of the calorimeter. It has been demonstrated that the modules with their central x<0 have on average larger gain correction factors, than modules with x>0. The value of their gains also tends to drift more with time than the modules with x>0. This can be seen in Figure 0.5. Evaluation of the gain correction factors is sensitive to the beam offset (position on the target) and the beam angle. The gain correction factors from two sides of the detector differ, and will converge into one value if the center of HyCal is moved artificially (in x or y). The alignment procedure corrects for the beam offset in x and y, but gains remain sensitive to the beam angle. Offset of 1 mm in x results in 1 % change of the gain correction value. More precise information on the beam position is needed, and can be obtained from from the BPMs and the photon profiler.

One of the main objectives of the study was to monitor the relative change of gains in time. In order to see this change, we plot gain correction factors vs group number, for several modules on both sides of the HYCAL central opening. As can be seen from Figure 0.5, the gains of the modules with x>0 change little with time, by 1-3 %. The crystals with x<0 show a very different behavior. The radiation incident occured between groups 4 and 5, and we observe a dramatic change, $\sim$ 15-20 %, in the gain correction factors between these two groups. It appears, that the modules begin to recover themselves from the radiation damage, and the difference in gain correction

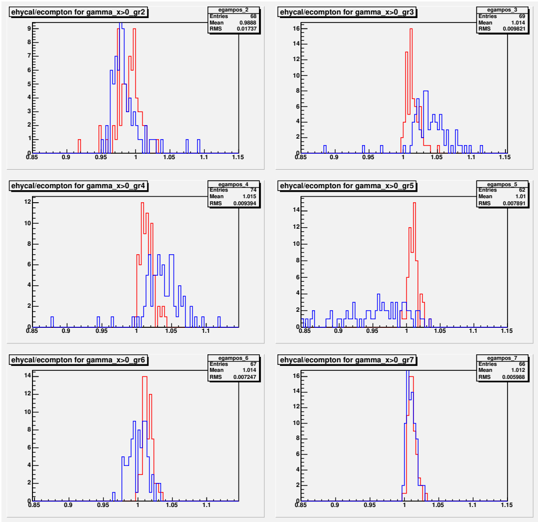

Figure 6: Distributions of gain correction factors, plotted separately for each group of runs for $x < 0$ (blue) and $x < 0$ (red). The asymmetry is particularly strong in group 5 (following the radiation incident); it is not seen in group 7 (closest to the last calibration

factors between groups 4 and 7 is on the order of $\sim$ 5-8 %.

The LMS gains follow a similar pattern, but are not identical quantitatively. More work needs to be done to understand how to use the LMS gains along with the gain correction factors. Figure 0.5 shows a comparison of the LMS gains with the gain correction factors, group by group.

The calibration procedure is carried out through several iterations. Once the first set of correction factors, $cf_i^{iter=1}$ is found, the corrections are applied to every module, i, and the procedure is repeated to obtain the next set of correction factors:

$$cf_i^{iter=2} = [\sum_{j}^{n-assoc} E_j/cf_j]/E_c, \tag{2}$$

where E_c is the total energy of the cluster expected from Compton kinematics, i is the calibrated module, E_j is the energy measured in every member cell j of the cluster with central id $= i$, $n - assoc$ is the number of member cells in the cluster with central id $= i$. The results converged after 4-5 iterations. In order to see the effect of this method of energy calibration, we plot the elasticity of the pairs, $(e_1 + e_2)/E_{beam}$ before and after the application of gain correction factors. The energies of the first and second clusters, e_1 and e_2 are found by summing over the energies of all cells of the cluster, corrected by the gain correction factor:

$$e_1 = \sum_{j}^{n-assoc} E_j/cf_j \tag{3}$$

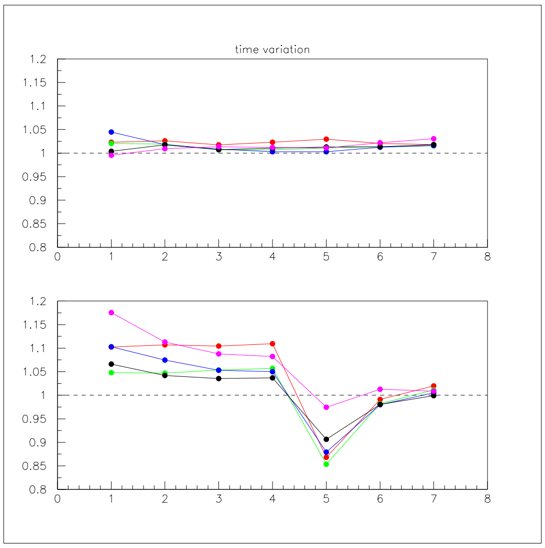

Figure 7: Colors correspond to different modules, x>0: 1487,1488,1489,1490,1491 (left plot), x<0: 1496,1497,1498,1499,1500 (right plot(. Gain correction factors are evaluated with respect to the last calibration for all groups.

The calibration procedure shifts the mean value of the peak closer to one, and reduces the standard deviation of the distribution. This is particularly evident in case of group 5, shortly after the radiation incident. The quantitative improvement in energy resolution will be summarized in a table below.

0.6 Calibration by matrix inversion

We also employed an alternative method of calibration, where gain correction factors are found simultaneously for all counters. In this method, the correction factors, c_i are found through the condition:

$$M = \sum_l (\sum_i c_i E_{il} - E_l)^2 = min, \tag{4}$$

where l is the event number, E_l is the energy expected for the cluster from Compton kinematics, and E_{il} is the energy deposited in a module i. This condition results in a system of linear equations:

$$\frac{dM}{dc_j} = \sum_l (\sum_i x_i E_{il} - E_i) E_{jl} = 0, \tag{5}$$

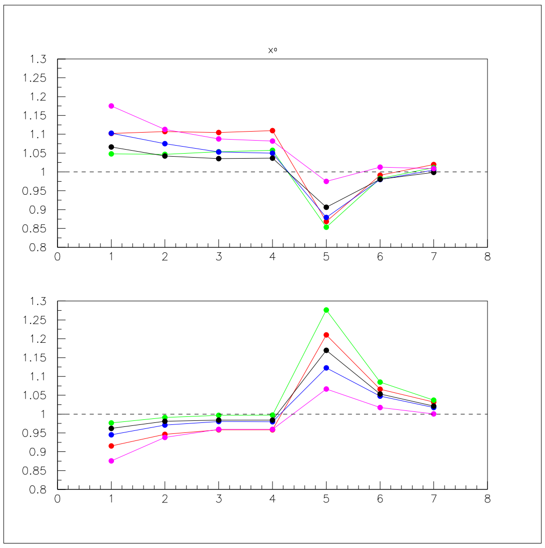

Figure 8: Gain correction factors for the five selected modules with x<0 are plotted vs group number (top plot), along with the LMS gains for these modules on the bottom plot)

which can be rewritten as

$$\sum_i c_i \sum_l \frac{E_{il} E_{jl}}{E_l^2} = \sum_l \frac{E_{jl}}{E_l} \tag{6}$$

In order to obtain correction factors c_i, we accumulate a 2156x2156 matrix $M_{ij} = \frac{E_{il} E_{jl}}{E_l^2}$, and a vector $V_j = \frac{E_{jl}}{E_l}$. The vector of correction factors, C_i is obtained by inverting the accumulated matrix M_{ij} and multiplying it by the vector V_j:

$$C_i = M_{ij}^{-1} * V_j \tag{7}$$

The counters that did not participate in the calibration process and the ones that were only exposed to the edges of the showers, resulting in small numeric values of energy, have corresponding diagonal elements of the matrix, and row of the vector V set to one. The non-diagonal elements of the rows corresponding to the counters with small amplitudes are set to zero. Once the correction factors are found, the new gains can be obtained:

$$g_i^{new} = g_i * c_i \tag{8}$$

The results of this method of calibration are compatible with the ones obtrained through the iteration method.

Gain correction factors from the two methods are compared, group by group, in Figure 0.6. The agree within 1-3%.

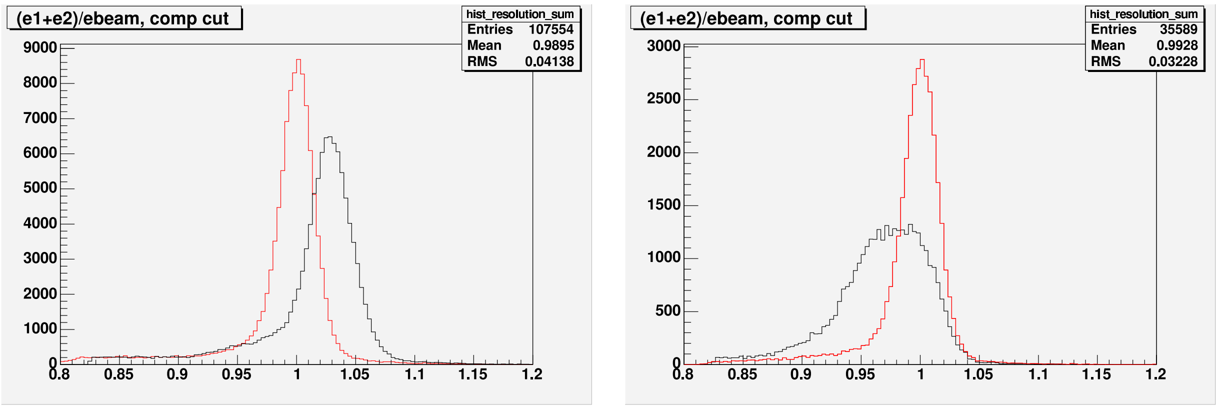

Figure 9: Left:$(e_1+e_2)/E_{beam}$ distribution before (black) and after (red) the calibration for group 4. Right: $(e_1+e_2)/E_{beam}$ distribution before (black) and after (red) the calibration for group 5

Table 2: Energy Resolution after the calibration by iteration, E>4.9 GeV

group number	Mean before	mean after	σ before	σ after	$\Delta\sigma$ (%)
1	1.018	1.011	0.0157	0.0147	~ 6
2	0.989	1.002	0.0184	0.0151	~ 18
3	1.029	1.001	0.0193	0.0154	~ 20
4	1.028	1.001	0.0188	0.0153	~ 19
5	0.983	1.001	0.0488	0.0147	~ 70
6	1.006	1.001	0.0168	0.0144	~ 14
7	1.013	1.001	0.0148	0.0144	~ 3

0.7 Gains obtained with beam energies 2-3 GeV and 4.9-5.5 GeV

During the experiment, compton data was accumulated in two beam energy ranges: 2-3 GeV and 4.9-5.5 GeV. Approximately 150 modules in the central part of HYCAL have enough statistics to result in two gains values: one for each energy range. For those modules that have both the low and high energy gain correction factors, we compare the two types of gain correction: $Low\_gain - High\_gain$. The distribution is shown on the left in Fig. 11 The average mean of these distributions is $0.003 - 0.006$. Gain correction factors are 1-3 % higher when obtained with the lower energy sample. This is due (at least, one of the reasons), to the energy non-linearity due to sparcification cut. More about non-linearity issues can be found at: $http://www.jlab.org/\ mochalov/hycal\_software/notes/linearity/Linearity\_1.html$ An em-

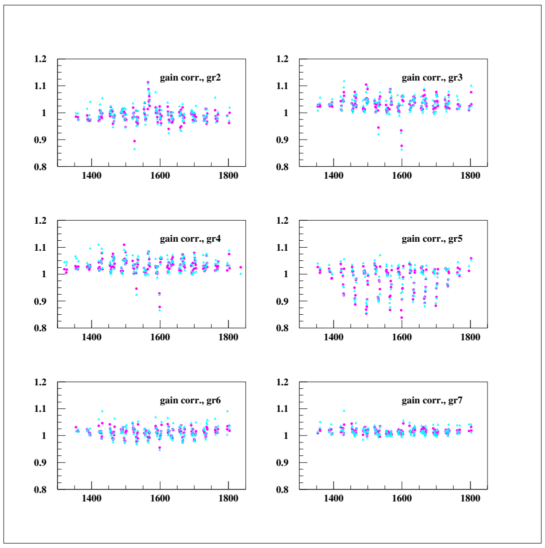

Figure 10: Gain correction factors vs module number, from the two methods of calibration.

pirical correction was applied to cluster energies:

$$\begin{aligned} E &\rightarrow E \times (1 + ecorr) \\ ecorr &= exp(-1.651 - 8.28E) + exp(-2.627 - 1.244 * E). \end{aligned} \quad (9)$$

This correction brings the two types of gains closer, as shown on the right in Fig. 11. New mean values are $0.0005 - 0.001$, which brings the difference between two types of gains to within a fraction of a percent. After demonstrating that the two types of gains are consistent, we can combine data of all beam energies to calculate one gain value for each module.

Table 3: Energy Resolution after the calibration by matrix inversion, E > 4.9 GeV

group number	Mean before	mean after	σ before	σ after	$\Delta\sigma$ (%)
1	1.018	1.005	0.0157	0.0157	0
2	0.989	1.001	0.0184	0.0149	$\sim$ 19
3	1.029	1.001	0.0193	0.0153	$\sim$ 21
4	1.028	1.000	0.0188	0.0156	$\sim$ 17
5	0.983	0.999	0.0488	0.0155	$\sim$ 68
6	1.006	1.000	0.0168	0.0148	$\sim$ 12
7	1.013	1.001	0.0148	0.0146	$\sim$ 2

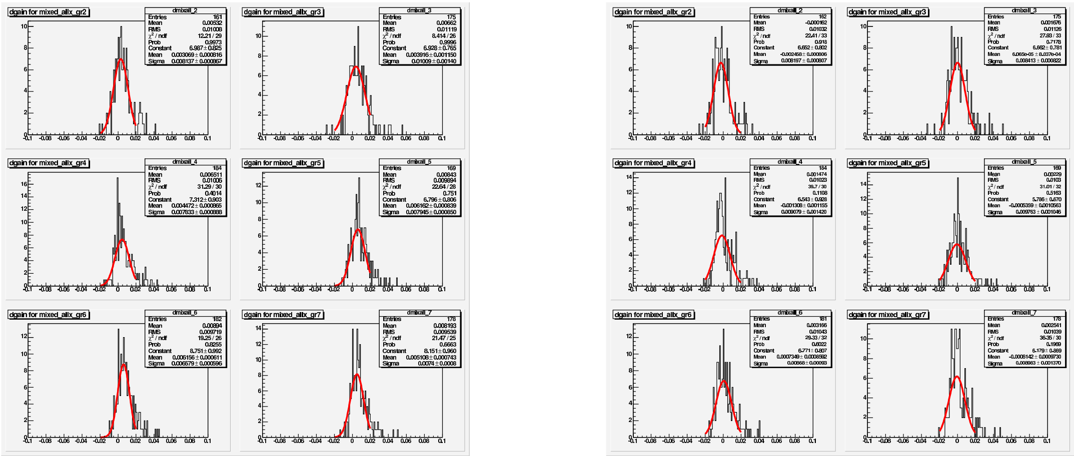

Figure 11: Left:Difference in gains obtained with beam energy 2-3 GeV and 4.9-5.5 GeV before the non-linearity correction. Right:Difference in gains obtained with beam energy 2-3 GeV and 4.9-5.5 GeV after the non-linearity correction

Table 4: Energy Resolution before and after calibration, all beam energies included

group number	Mean before	mean after	σ before	σ after
1	1.323	1.011	0.0257	0.0142
2	1.286	1.003	0.0316	0.0154
3	1.273	1.002	0.0330	0.0160
4	1.273	1.001	0.0330	0.0159
5	1.258	1.002	0.0814	0.0180
6	1.264	1.002	0.0404	0.0178
7	1.268	1.002	0.0381	0.0178

0.8 Final results and how to use them

In the final procedure, initial gains were set to 1, and new gains were obtained without the use of snake scan data. Since no initial gains were used, the initial resolution distribution $(e_1 + e_2)/ebeam$ was centered around 1.2-1.3. After the new gains were applied, the distribution became centered at 1. The plots are shown in Fig. 0.8. The change in the width of resolution distributions is listed in Table 0.8.

New gains obtained through the iteration method were loaded into the calibration database under system = crystal, attribute = compton_gain. The modules that didnot have sufficient statistics to produce a gain value regain their snake calibration values: from snake 1 if run numbers is < 4828, and snake 2 otherwise. In order to use Compton gains instead of the snake scan gains, a flag, $DCOMPTON\_GAINS$, needs to be

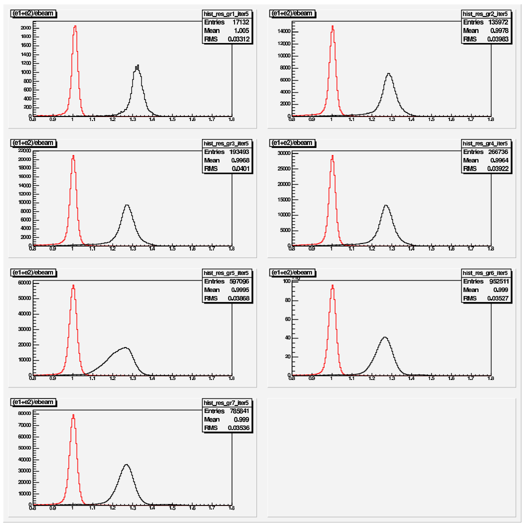

Figure 12: Energy resolution before (black) and after (red) the application of new gains.

set to 1 in *include/hycal.h* file: *#define DCOMPTON_GAINS* 1. Subroutine *hycal/hycal_brun.cc* has been modified to incorporate this option.

The geometric availability of compton gains is shown in Fig. 13 and 14. The colors on this plot are indicative of the change in gains between the last snake scan and the compton gains obtained from a given group of runs. Modules shown in white do not have compton gains.

0.9 Effect of new gains on the energy resolution in production data

The effect of new gains was tested by looking at the plots of $(e_1 + e_2)/ebeam$ using 2-cluster events in the production data on carbon and lead. The following runs were used: 1)Lead runs 5084-93 (used skim files from
/mss/hallb/primex/skim/october_2004/pi0_pass2/)
2)Carbon runs 5159-5166 (used skim files from
/mss/hallb/primex/skim/october_2004/pi0_pass2/)

Events with 2 clusters only were selected, where the invariant mass of two clusters is between 0.095 GeV and 0.300 GeV, and x and y of the clusters less than 30 cm (crystal part only). The distributions are shown in Fig. 15 (for the lead target) and Fig. 16 for the carbon target. The peak of the distributions was fitted with a gaussian function, and its sigma taken as energy "resolution".

Conclusion: Using double arm compton gains significantly improved energy resolu-

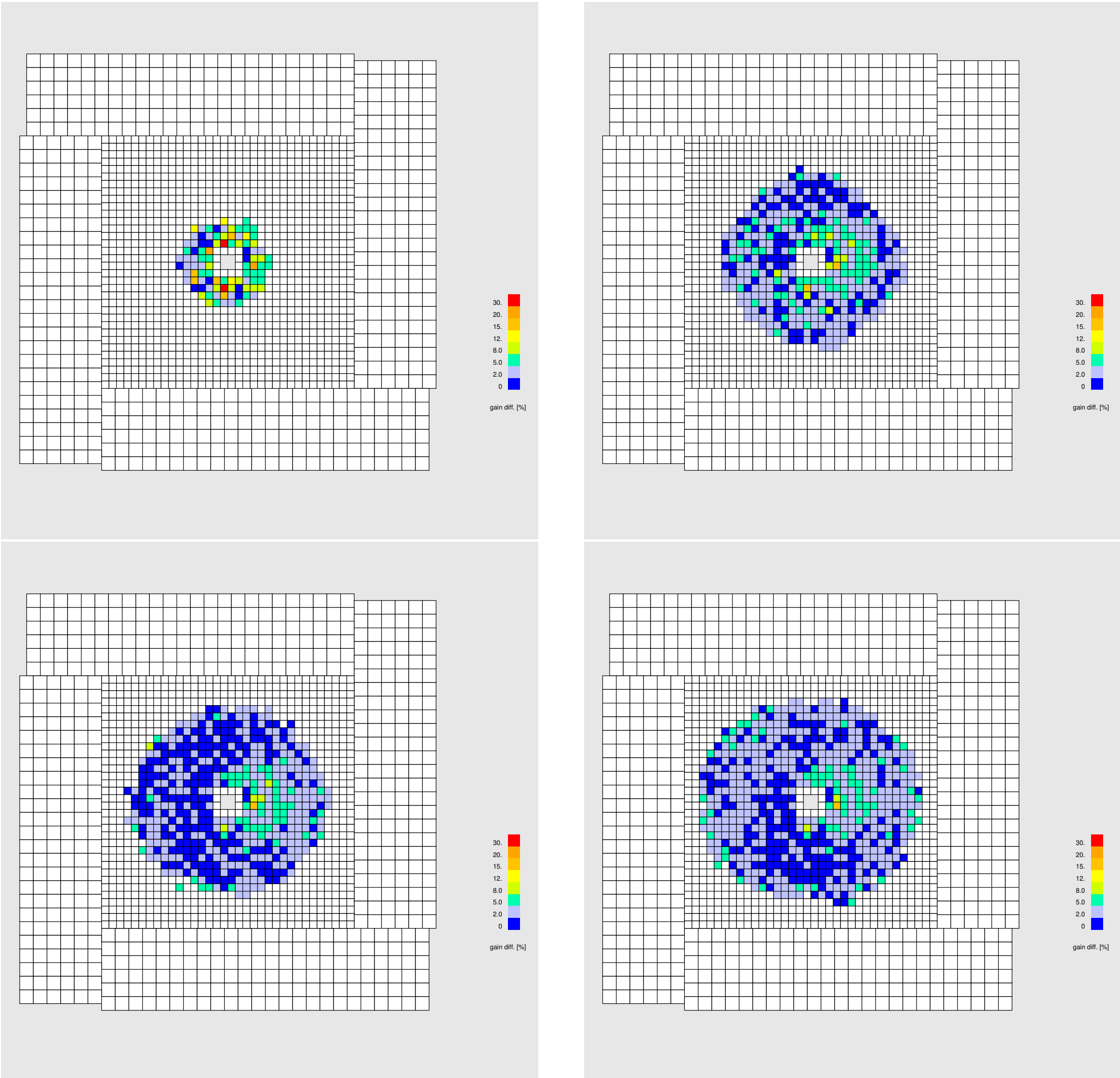

Figure 13: Geometric coverage on HYCAL and difference in % between the new compton gains and the last snake scan gains for groups 1-4.

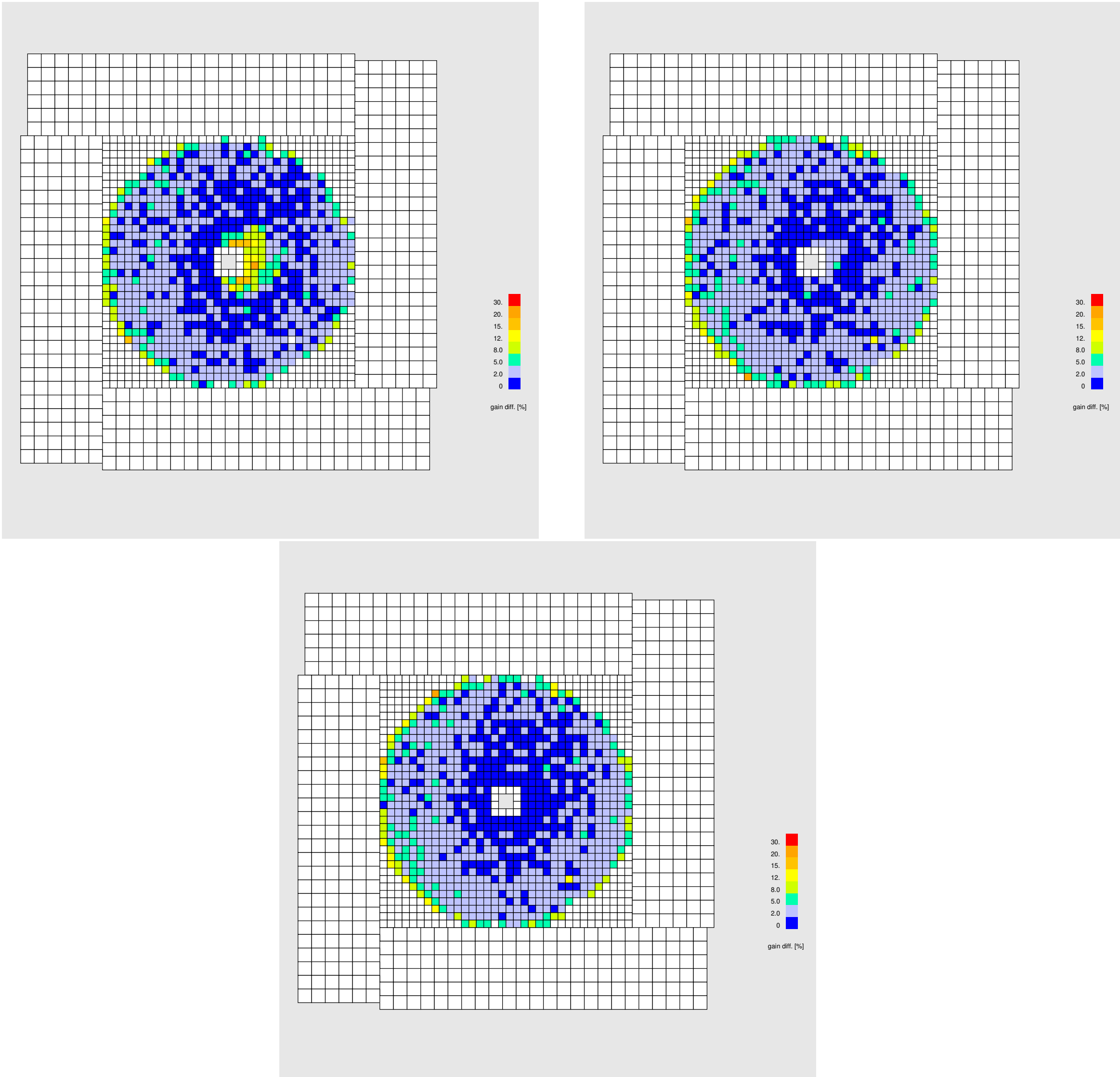

Figure 14: Geometric coverage on HYCAL and difference in % between the new compton gains and the last snake scan gains for groups 5-7.

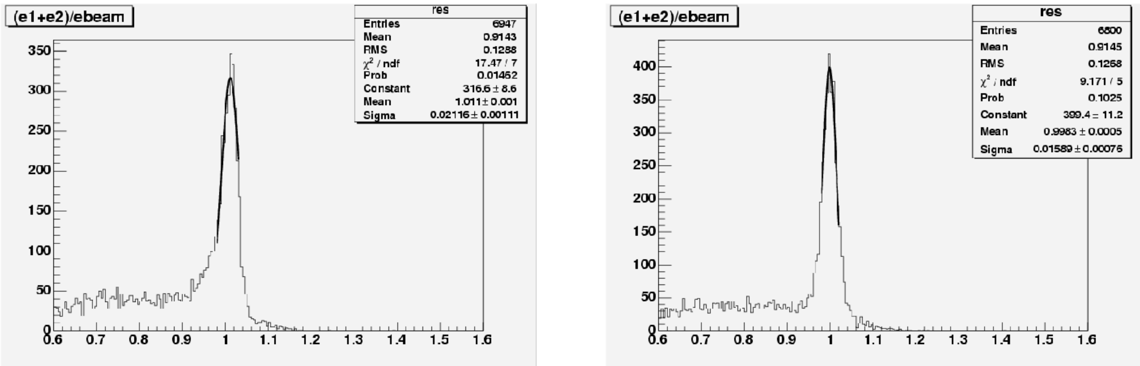

Figure 15: Lead Target. Left:Energy resolution with "snake" gains. Right: Energy resolution with "DCOMP" gains.

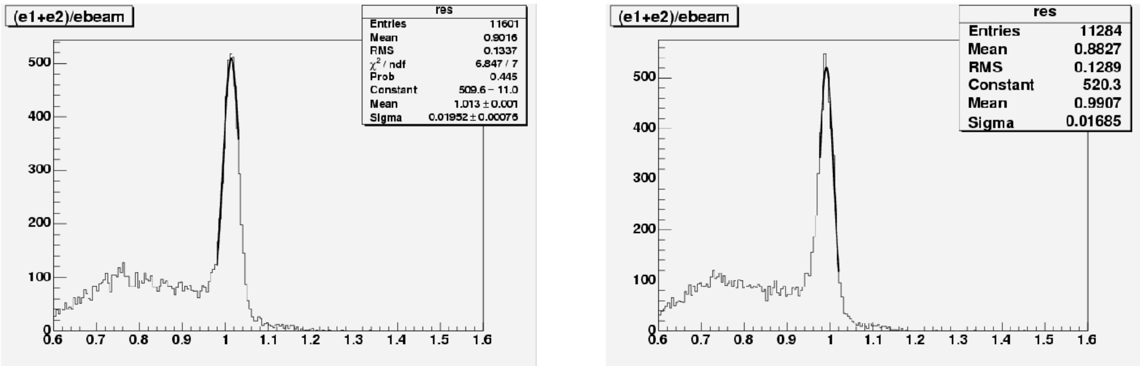

Figure 16: Carbon Target. Left:Energy resolution with "snake" gains. Right: Energy resolution with "DCOMP" gains.

tion (from 2.1 % to 1.6 %)for a group of lead runs 5084-5096 (these were taken shortly after the radiation accident). There is also some improvement in energy resolution (from 2% to 1.7%) for carbon runs 5159-5166.